JOURNAL OF SOLID STATE CHEMISTRY **91**, 61–70 (1991)

A New Preparation Method of $LaMnO_3$ Perovskite Using Electrochemical Oxidation

TAKESHI SASAKI, YASUMICHI MATSUMOTO, JUKICHI HOMBO, AND YORIYUKI OGAWA

Department of Applied Chemistry, Faculty of Engineering, Kumamoto University, Kurokami 2-39-1, Kumamoto 860, Japan

Received July 16, 1990; in revised form October 24, 1990

$LaMnO_3$ perovskite was prepared by heat treatment of an oxide film which was electrochemically deposited on a Pt electrode in solutions containing both La^{3+} and Mn^{2+} ions. The La/Mn ratio in the deposited oxide films increased with an increase in the $[La^{3+}]/[Mn^{2+}]$ ratio in solution and with a positive shift of electrode potential. The maximum value in this ratio was about one, and was obtained in solution with $[La^{3+}]/[Mn^{2+}] > 500$ and/or in a potential region more positive than about 1.9 V vs. Ag/AgCl. It was presumed from IR, TG, XRD, and XPS measurements that the incorporation of La^{3+} ion into the oxide film during electrochemical deposition is based on a specific adsorption of La^{3+} ions onto the surface of amorphous and hydrous ε-MnO_2, which has some oxygen deficiencies, and that the La^{3+} ion exists as a hydroxide in the oxide. A single phase of $LaMnO_3$ perovskite was obtained by heat-treatment of the deposited oxide film with La/Mn $\doteqdot$ 1.0 at a temperature higher than about 750°C, which was always lower than the preparation temperature in the ceramic technique (about 1200°C). The crystallization process in the heat treatment was also discussed from TG and XRD analysis.

Introduction

It is well known that an oxide film can be anodically prepared on a metal substrate, where the metal electrochemically dissolves as a cation into solution, followed by some chemical reactions with OH^- and/or H_2O in the solution. In this case, a complex oxide film can be synthesized if the solution contains other metal cations. From this point of view, we have electrochemically synthesized iron spinel oxide $Fe_{3-x}Li_xO_4$, where the solution contains Li^+ ion (*1*). From a similar point of view, $LaCrO_3$ (*2*), $LiNbO_3$, and $BaTiO_3$ (*3*) were also electrochemically synthesized. The electrochemical synthesis of complex oxide film has the following two advantages compared with other methods such as CVD and sputtering etc. One is that the film can be easily prepared with a simple apparatus and under simple conditions. The other is that the film thickness and the grain size of the oxide can be controlled with the quantity of electricity and the current density, respectively.

$LaMnO_3$ is suitable as an air electrode material for high temperature solid oxide fuel cells (SOFC), because of its chemical stability at high temperature, electrocatalytic property, high electron conductivity, and thermal expansion match with the solid oxide electrolyte, yttria-stabilized zirconia (*4*). For use as an air electrode in a SOFC, the cathode must be thin and porous, so that

0022-4596/91 $3.00

oxygen easily diffuses onto the electrolyte (*5*). Some preparation methods for the thin and porous films of $LaMnO_3$ have been studied (*6*).

It is well known that manganese oxide can be directly synthesized on an electrode by anodic oxidation in a solution containing Mn^{2+} ion. Therefore, it may be possible to form $LaMnO_3$ films by anodic oxidation, if the solution contains both metal cations Mn^{2+} and La^{3+}, as in the preparation case of $Fe_{3-x}Li_xO_4$ (*1*). In this paper, a new preparation method of the $LaMnO_3$ film using electrochemical oxidation is demonstrated and its mechanism is discussed.

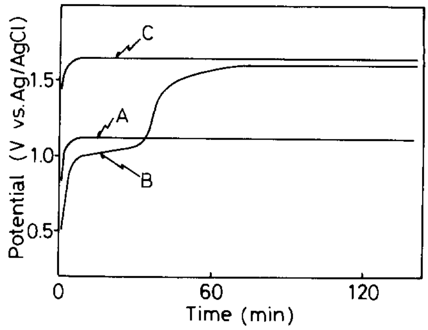

FIG. 1. Time dependences of the Pt electrode potential under galvanostatic electrolysis of 0.5 mA cm^{-2} in solutions with the $[La^{3+}]/[Mn^{2+}]$ ratios of 10 (A), 50 (B), and 1000 (C).

Experimental

Pt plates (99.9%, 10 × 10 mm) were used as the working and counter electrodes, and a Ag/AgCl electrode was used as the reference. Electrode potential was referred to Ag/AgCl unless otherwise stated. The electrolytes were $Mn(NO_3)_2$ and $La(NO_3)_3$ in aqueous solutions, whose total concentration ($[La^{3+}] + [Mn^{2+}]$) was always 1 *M*. Both galvanostatic and potentiostatic electrolysis were carried out for 3 hr at room temperature. In the case of the galvanostatic electrolysis, current density was kept constant at 0.5 mA cm^{-2}. The oxide films prepared on the electrode were washed with distilled water, followed by drying at room temperature. The as-deposited oxide films were examined by infrared absorption spectroscopy (IR), thermal gravimetry (TG), and X-ray photoelectron spectroscopy (XPS). All the samples were heated in air at various temperatures for 4 hr for the purpose of crystallization, since the as-deposited oxide films prepared at room temperature were always amorphous. The structures of the oxide films after the heat-treatment were examined by X-ray diffraction analysis (XRD) with monochromatic Cu*K*α radiation. Morphological observations of the oxide films were carried out by a scanning electron microscope (SEM). The oxide films were dissolved into HCl and then analyzed by inductively coupled plasma (ICP) spectroscopy to determine the atomic ratios of La/Mn in the oxide films.

Results and Discussion

Galvanostatic Synthesis

Figure 1 shows some typical time dependences of the electrode potential under galvanostatic electrolysis in the solutions consisting of the various ratios of $[La^{3+}]/[Mn^{2+}]$. The variation of potential with time was dependent on the $[La^{3+}]/[Mn^{2+}]$ ratio in the solution, where two plateaus of about 1.0–1.1 V and 1.6–1.65 V were observed, as shown in Fig. 1. In general, type A and type C curves in this figure were observed in the solutions with the low (<10) and high (>500) ratios of $[La^{3+}]/[Mn^{2+}]$, respectively. Reactions at 1.0–1.1 V and 1.6–1.65 V are mainly based on MnO_2 production and O_2 evolution respectively, since O_2 evolution was observed at the latter potential. The amounts of La^{3+} ions contained in the oxide films prepared at high potential (1.6–1.65 V) were always larger than those in the oxide films prepared at low potential (1.0–1.1 V), suggesting that the incorporation of La into the

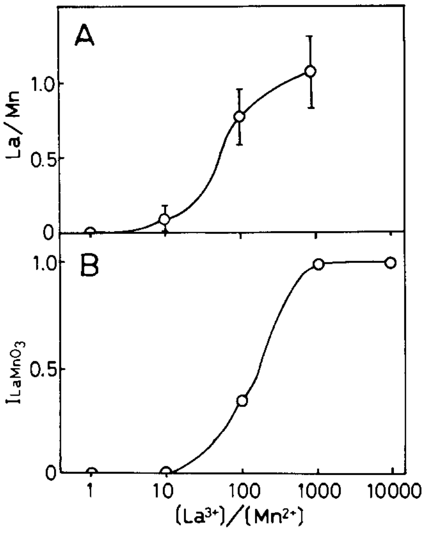

FIG. 2. Atomic ratio of La/Mn in the oxide film (A) and I_{LaMnO3} (B), as a function of the $[La^{3+}]/[Mn^{2+}]$ ratio in solution.

oxide film depends on the electrode potential as well as the $[La^{3+}]/[Mn^{2+}]$ ratios as described below.

Figure 2A shows the atomic ratio of La/Mn in the oxide film which was analyzed by using ICP spectroscopy as a function of the $[La^{3+}]/[Mn^{2+}]$ ratio in the solution. The atomic ratio of La/Mn in the oxide increases with an increase in the $[La^{3+}]/[Mn^{2+}]$ ratio in the solution, but saturates to 1 at an ionic ratio of 1000. The oxide film deposited in the solution with the $[La^{3+}]/[Mn^{2+}]$ ratio of 1000 corresponded to the La/Mn atomic ratio in $LaMnO_3$, but was amorphous, because no peaks were observed in the X-ray diffraction pattern. After heat-treatment at 1000°C, single phase $LaMnO_3$ was observed for the $[La^{3+}]/[Mn^{2+}]$ ratio >1000. The importance of the cation ratio in solution is illustrated in Fig. 3, which shows typical X-ray diffraction patterns of the heat-treated oxide films at 1000°C. Samples A and B in this figure were prepared in the solutions with the $[La^{3+}]/[Mn^{2+}]$ ratios of 1000 and 100, respectively. As can be seen, sample A consisted of the single phase of $LaMnO_3$, while sample B consisted of a mixture of Mn_3O_4 and $LaMnO_3$. For the intensities in Fig. 3, the following equation was used for the purpose of qualitative evaluation of the degree of $LaMnO_3$ formation in the oxide film,

$$I_{\mathrm{LaMnO3}} = I_{\mathrm{LaMnO3(100)}}/(I_{\mathrm{LaMnO3(100)}} + I_{\mathrm{Mn3O4(211)}}), \quad (1)$$

where $I_{\mathrm{LaMnO3(100)}}$ and $I_{\mathrm{Mn3O4(211)}}$ are the intensities of the (100) diffraction peak of $LaMnO_3$ perovskite and of the (211) diffraction peak of Mn_3O_4, respectively. I_{LaMnO3} as a function of the $[La^{3+}]/[Mn^{2+}]$ ratio in solution in the electrolysis is shown in Fig. 2B. As a matter of course, a single phase of $LaMnO_3$ was obtained for the oxide with the La/Mn ratio of 1.

Figures 4A and 4B are SEM micrographs of the as-deposited oxide film with the La/Mn atomic ratio of 1 and the 1000°C heat-treated oxide film, respectively. The thickness of this as-deposited oxide film and the heat-treated oxide film was about 3–4 μm and 2–3 μm, respectively. The grain size of the latter film was 1–2 μ. The amount of La in the as-deposited oxide film was significantly decreased by immersion for 30 min in water immediately after the electrolysis.

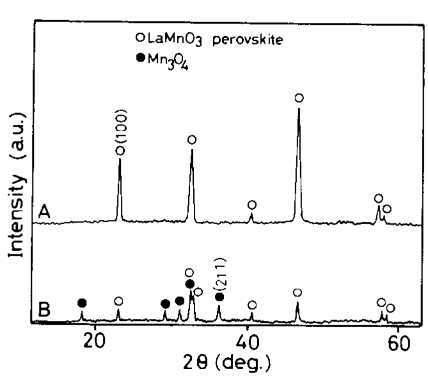

FIG. 3. X-ray diffraction patterns of the heat-treated oxide films at 1000°C. The films were prepared in solution with $[La^{3+}]/[Mn^{2+}]$ ratios of 1000 (A) and 100 (B).

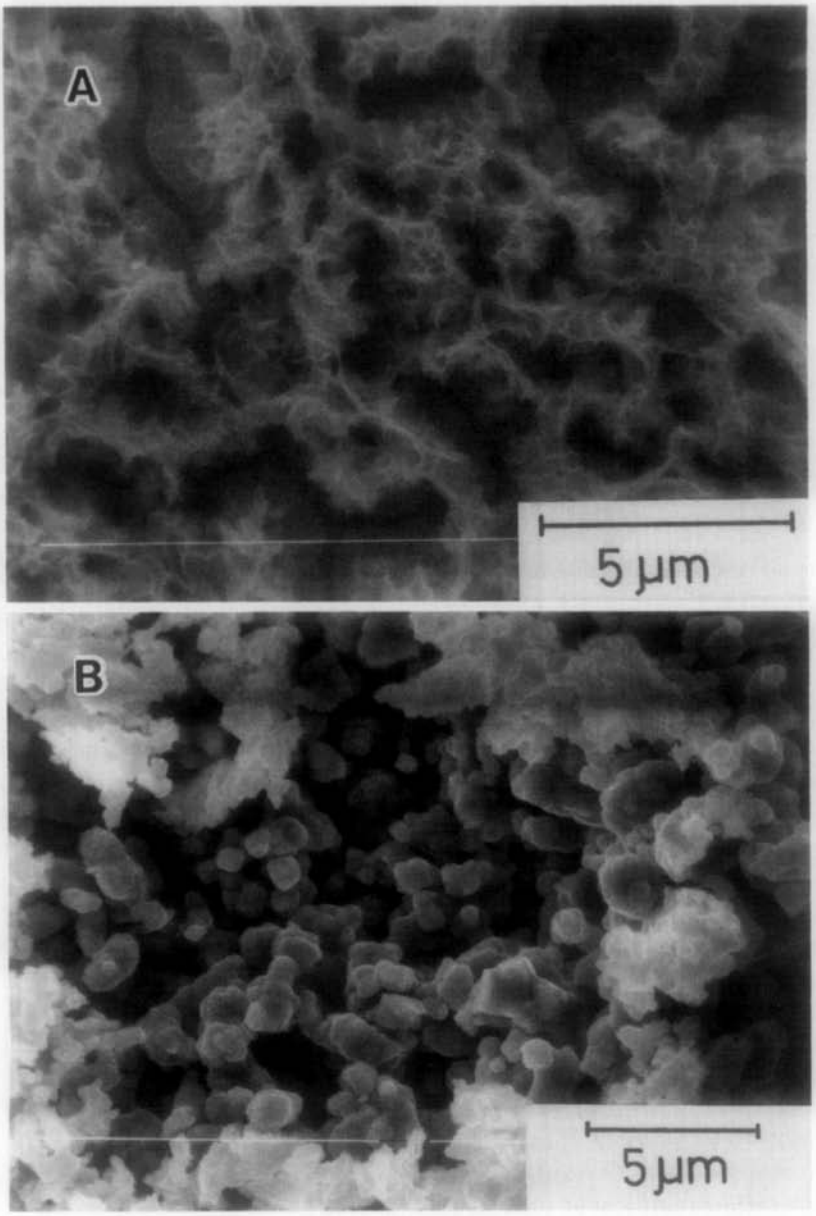

FIG. 4. SEM micrographs of the as-deposited oxide film prepared by the galvanostatic synthesis in solution with the $[La^{3+}]/[Mn^{2+}]$ ratio of 1000 (A) and its heat-treated oxide film at 1000°C (B).

Figure 5 shows the atomic ratio of La/Mn in the oxide film after the immersion, as a function of the $[La^{3+}]/[Mn^{2+}]$ ratio in the solution. This decrease indicates that La in the as-deposited oxide film easily dissolves in water, and, therefore, may suggest the simple adsorption of La^{3+} ion onto the deposited MnO_2 as the deposition mechanism of La^{3+} ions. In order to evaluate the contribution of simple adsorption of La^{3+} ion to the incorporation, MnO_2 films which were prepared in 0.01 M $Mn(NO_3)_2$ solution by

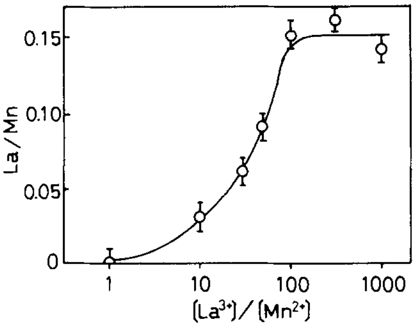

FIG. 5. Atomic ratio of La/Mn in the oxide film after immersion in water for 30 min, as a function of the $[La^{3+}]/[Mn^{2+}]$ ratio in solution.

the galvanostatic electrolysis were immersed in 1 *M* $La(NO_3)_3$ solution for 3 hr. The concentrations of Mn^{2+} and La^{3+} ions in the above solutions correspond to those in the electrolyte with the $[La^{3+}]/[Mn^{2+}]$ ratio of 100. The MnO_2 film was washed with water and then analyzed with ICP spectroscopy. The atomic ratio of La/Mn in this oxide was less than about 0.1. This value was very small compared with that (0.8) in the oxide film electrochemically prepared in the solution with the $[La^{3+}]/[Mn^{2+}]$ ratio of 100. This result suggests that the incorporation of La^{3+} ion into the oxide can not be based on simple adsorption but must involve specific adsorption with weak chemical bonds.

Potentiostatic Synthesis

The typical time dependence of current density is illustrated in Fig. 6, where the Pt electrode was held at 1.8 V in the solution with the $[La^{3+}]/[Mn^{2+}]$ ratio of 1000. A decrease of the current density in the initial stage in this figure is due to the Pt electrode surface being covered with the oxide film, indicating that the conductivity of the deposited oxide film is low.

Figure 7 shows the La/Mn ratios in the oxide films deposited in the solutions with the $[La^{3+}]/[Mn^{2+}]$ ratio of 10 (A) and 100 (B), as a function of the electrode potential applied in electrolysis. In the case of galvanostatic electrolysis in the solution with the $[La^{3+}]/[Mn^{2+}]$ ratio of 10, where the electrode potential was about 1.1 V, the atomic ratio of La/Mn in the deposited oxide film was about 0.1 (Fig. 2A).On the other hand, in potentiostatic elecrolysis, the atomic ratios of La/Mn in the prepared oxide films are larger than about 0.4, when the electrode potential is more positive than about 1.9 V. Thus, the La content in the oxide film increases as the applied potential becomes more positive. Figure 8 shows SEM micrographs of the as-deposited oxide films prepared at various potentials in the solution with the $[La^{3+}]/[Mn^{2+}]$ ratio of 10. The morphology of the as-deposited oxide largely depends on the applied potential. In general, for the oxide deposited under high current density, the particle size and the surface area are small and large, respectively. Therefore, the oxide prepared under this condition can easily react with some cations, which can explain the potential dependence of the atomic ratio of La/Mn seen in Fig. 7, because the current density increases with the positive shift of applied potential.

Crystallization Process

Figure 9 shows the X-ray diffraction pattern of the as-deposited oxide film which

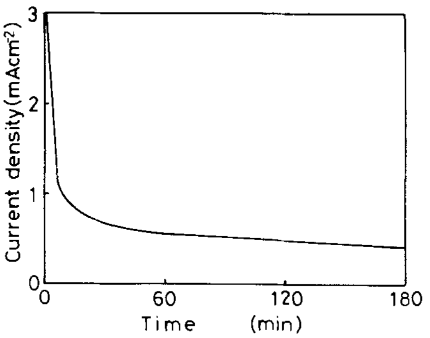

FIG. 6. Time dependence of current density where the Pt electrode was held at 1.8 V in solution with an $[La^{3+}]/[Mn^{2+}]$ ratio of 1000.

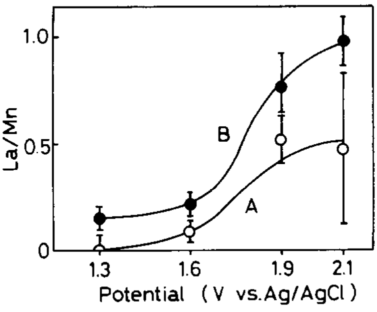

FIG. 7. Atomic ratios of La/Mn in the oxide films prepared under potentiostatic electrolysis, as a function of the applied potential. A and B denote the electrolytes with $[La^{3+}]/[Mn^{2+}]$ ratios of 10 and 100, respectively.

was prepared by galvanostatic synthesis in a (0.1 M $Mn(NO_3)_2$ solution in an autoclave at 150°C under pressure of 1×10^6 Pa. The sharp X-ray diffraction peaks indicate that the crystallization occurred during the deposition process at 150°C. The X-ray diffraction pattern of the film was identified to be ε-MnO_2. X-ray diffraction patterns similar to that in Fig. 9 were obtained for the as-deposited oxide films prepared in the solution containing both La^{3+} and Mn^{2+} ions at 150°C. Consequently, the as-deposited oxide films prepared at room temperature are presumed to be similar to ε-MnO_2 containing La^{3+} ion in structure, although this is amorphous.

Figure 10 shows the typical infrared absorption spectra of the as-deposited oxide films which were prepared under 2.1 V in 0.1 M $Mn(NO_3)_2$ solution (A) and in the solution with the $[La^{3+}]/[Mn^{2+}]$ ratio of 10 (B). The absorption band (a) was assigned to the O–H stretching vibration of hydroxyl groups on the oxide surface, and the absorption band (b) was assigned to the O–H stretching vibration of adsorped water (*7, 8*). It should be noted that the absorption band (a) in the spectrum A is relatively smaller than that in the spectrum B. This indicates that a large amount of the hydroxyl groups are present in the as-deposited oxide containing La^{3+} ion, suggesting that La^{3+} ion will exist as a hydroxide in the as-deposited oxide. The x-ray photoelectron spectra of $Mn2p_{3/2}$ level were also measured to evaluate the valence of Mn in the as-deposited oxide films prepared in solutions containing both La^{3+} and Mn^{2+} ions. These peak positions for all samples were same as that of MnO_2 (641.9 eV), suggesting that the Mn in the oxide films exists as Mn^{4+}. This supports the idea that the as-deposited oxide films consist of an amorphous and hydrous MnO_2 with lanthanum hydroxide.

Figure 11 shows the thermogravimetric (TG) and differential thermogravimetric (DTG) curves of the oxide films prepared under 2.1 V in 0.1 M $Mn(NO_3)_2$ solution (A) and in solution with a $[La^{3+}]/[Mn^{2+}]$ ratio of 10 (B). According to a previous thermogravimetric study of electrochemically deposited MnO_2 (*9*), some of the weight changes in Fig. 11A can be characterized as follows. A weight loss at temperatures below 130°C is due to the evaporation of water adsorbed on the oxide. The subsequent gradual weight loss between 130 and 500°C is mainly due to desorption of bonding water. Weight losses at 550 and 950°C are based on the formation of Mn_2O_3 and Mn_3O_4, respectively. Therefore, the value of x in MnO_x and the water content in the as-deposited oxide were estimated from the TG curve in Fig. 11A to give the composition $MnO_{1.8} \cdot 1.5H_2O$.

The TG–DTG curves in B are different in shape from those in A, although at temperatures below 130°C similar weight loss due to the evaporation of water was observed. A broad peak at about 250°C in the DTG curve in B probably comes from the decomposition of $La(OH)_3$ in the as-deposited MnO_2, because $La(OH)_3$ decomposes to LaO(OH) at 200–300°C (*10, 11*). That is, a large amount of OH groups are present in the as-deposited oxide containing La. This result is in harmony with those observed for the

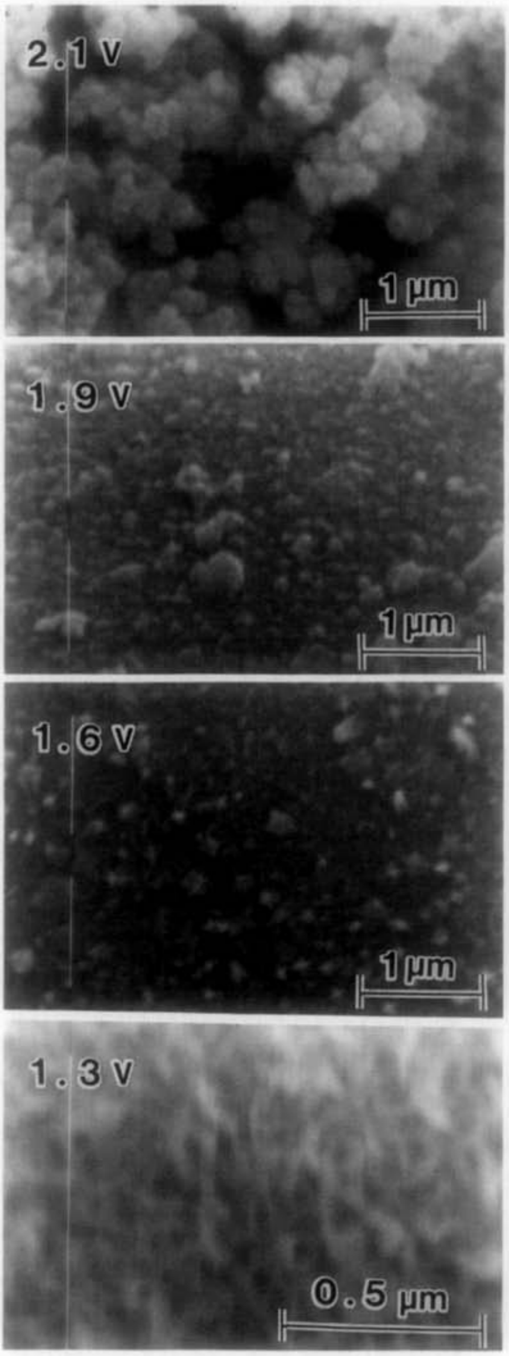

FIG. 8. SEM micrographs of the as-deposited films prepared at various potentials (1.3–2.1 V) in solution with an [La^{3+}]/[Mn^{2+}] ratio of 10.

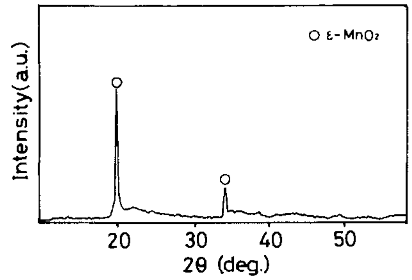

FIG. 9. X-ray diffraction pattern of the as-deposited oxide film which was prepared by the galvanostatic synthesis in 0.1 *M* $Mn(NO_3)_2$ solution at 150°C under pressure of 1×10^6 Pa.

IR spectrum. Consequently, we conclude that amorphous MnO_2 containing La will be electrochemically deposited as follows,

$$Mn^{2+} + mH_2O \rightarrow MnO_{2-x} \cdot nH_2O + (2m - 2n)H^+ + (2m - 2n)e^- \quad (1)$$

$$MnO_{2-x} \cdot nH_2O + La^{3+} + 3H_2O \rightarrow MnO_{2-x} \cdot nH_2O \cdot La(OH)_3 + 3H^+ \quad (2)$$

where m equals $2 - x + n$ and the value of n must be near 1.5. $La(OH)_3$ will specifically adsorb onto MnO_{2-x} in such a way that the La/Mn ratio is one.

Figure 12 shows the X-ray diffraction patterns of the oxide films heated at various temperatures, which were prepared by the galvanostatic synthesis in the solution with the $[La^{3+}]/[Mn^{2+}]$ ratio of 1000 so that their La/Mn ratios were about one. No diffrac-

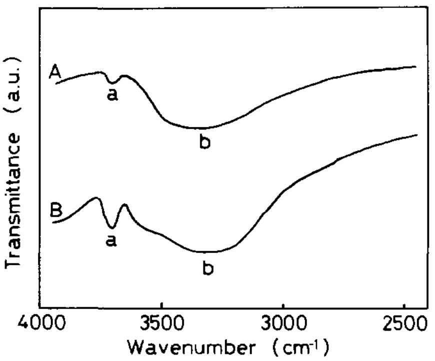

FIG. 10. Infrared spectra of the as-deposited oxide films which were prepared at 2.1 V in 0.1 *M* $Mn(NO_3)_2$ solution (A) and in solution with the $[La^{3+}]/[Mn^{2+}]$ ratio of 10 (B).

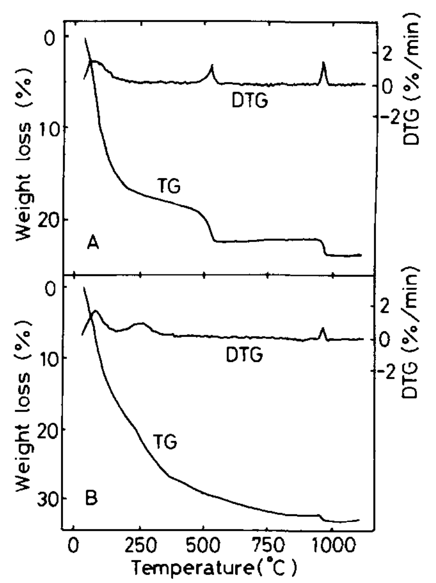

FIG. 11. TG–DTG curves of the oxides prepared at 2.1 V in 0.1 *M* $Mn(NO_3)_2$ solution (A) and in solution with the $[La^{3+}]/[Mn^{2+}]$ ratio of 10 (B).

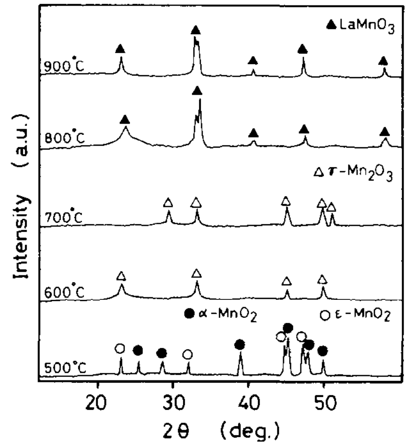

FIG. 12. X-ray diffraction patterns of the oxides heated at various temperatures. All the samples were prepared in solution with an $[La^{3+}]/[Mn^{2+}]$ ratio of 1000.

tion peaks were observed for the samples heated at temperatures below 400°C. As shown in Fig. 12, crystallization of MnO_2 occurs at about 500°C. The change of MnO_2 to Mn_2O_3 at 600°C agrees with the result in weight loss in TG (Fig. 11A). However, this result was not clearly observed for the oxide containing La (Fig. 11B). It may be that the x in MnO_{2-x} will be larger for the oxide containing La, leading to a smaller weight loss when the structure changes from MnO_2 to Mn_2O_3.

$LaMnO_3$ was observed by heat-treatment at 800°C. That is, $LaMnO_3$ perovskite was formed at a temperature range of 750–800°C. No weight loss in the formation of $LaMnO_3$ in this temperature range (Fig. 11B) indicates that $LaMnO_3$ is produced by a no weight loss reaction between Mn_2O_3 and La_2O_3. Consequently, the processes of $LaMnO_3$ perovskie formation from the oxide films containing La (La/Mn = 1) are summarized as follows,

$$MnO_{2-x} \cdot nH_2O \cdot La(OH)_3 \xrightarrow{200^\circ C} MnO_{2-x} \cdot La(OH)_3, \tag{3}$$

$$MnO_{2-x} \cdot La(OH)_3 \xrightarrow{200-300^\circ C} MnO_{2-x} \cdot LaO(OH), \tag{4}$$

$$MnO_{2-x} \cdot LaO(OH) \xrightarrow{450-550^\circ C} MnO_{2-x} \cdot \tfrac{1}{2}La_2O_3, \tag{5}$$

$$MnO_{2-x} \cdot \tfrac{1}{2}La_2O_3 \xrightarrow{500-600^\circ C} Mn_2O_3 \cdot La_2O_3, \tag{6}$$

$$Mn_2O_3 \cdot La_2O_3 \xrightarrow{750-800^\circ C} LaMnO_3. \tag{7}$$

In this process, bonding water in the oxide is neglected as a matter of convenience, although some bonding water will be released in the temperature range of 200–500°C. No diffraction peaks for La compounds such as $La(OH)_3$, $LaO(OH)$, and La_2O_3 were observed in Fig. 12, indicating that they exist as amorphous or very small particles. According to Refs. (*10*) and (*11*), Reaction (4) must also proceed, although a distinct weight loss was not observed in the TG curve. The gradual weight loss at the temperature range 250–700°C in Fig. 11B suggests that processes (3–7) continuously occur in the oxide film.

Summary

$LaMnO_3$ perovskite films (2–3 μm thick) were prepared by heat-treatment of oxides which were electrochemically deposited on a Pt electrode in solution containing both La^{3+} and Mn^{2+} ions. The La/Mn atomic ratio in the deposited oxide film strongly depends on the $[La^{3+}]/[Mn^{2+}]$ ratio in the solution and electrode potential. The maximum value of the La/Mn atomic ratio obtained was about 1, which corresponds to the cation ratio in $LaMnO_3$, in solution with $[La^{3+}]/[Mn^{2+}] > 500$, and/or in a potential region more positive than about 1.9 V vs Ag/AgCl. From IR, TG, XRD, and XPS measurements, the as-deposited oxide with an La/Mn atomic ratio of 1 was presumed to be amorphous and hydrous MnO_2 which contained La^{3+} ions by specific adsorption, such as $MnO_{2-x} \cdot 1.5H_2O \cdot La(OH)_3$. It was also found that the as-deposited oxide was dehydrated to MnO_2 and $LaO(OH)$ at 200–300°C and then decomposed to Mn_2O_3 and La_2O_3 at 450–600°C. $LaMnO_3$ was finally formed by reaction of Mn_2O_3 with La_2O_3 at temperatures higher than 750°C. This is a new preparation method of $LaMnO_3$ film at relatively low temperature, whose composition can be controlled by electrode potential.

Acknowledgment

The authors are grateful for the ICP analysis carried out by the laboratory of Prof. H. Egawa.

References

1. Y. Matsumoto, J. Hombo, and C. Qiong, *J. Electroanal. Chem.* **279**, 331 (1990).
2. H. Konno, M. Tokita, and R. Furuichi, *J. Electrochem. Soc.* **137**, 361 (1990).
3. M. Yoshimura and S. Somiya, *Proc. Int. Symp. Sci. Tech. Sinter.* **1**, 108 (1987).
4. A. Hammouche, E. Siebert, and A. Hammou, *Mater. Res. Bull.* **24**, 367 (1989).
5. J. Mizusaki, H. Tagawa, K. Tsuneyoshi, K. Mori, and A. Sawata, *Nippon Kagaku Kaisi*, 1623 (1988).
6. H. Michibata, T. Namikawa, and Y. Yamazaki, *Denki Kagaku* **57**, 1010 (1989).
7. O. Glemser and E. Hartert, *Z. Anorg. Allgem. Chem.* **283**, 111 (1956).
8. J. M. Serratsa, Proceedings of the 9th National Clay Conference, Pergamon Press, London (1961).
9. A. Era, Z. Takehara, and S. Yoshizawa, *Denki Kagaku* **35**, 334 (1967).
10. R. C. Rau and W. J. Glover, Jr., *J. Amer. Ceram. Soc.* **47**, 382 (1964).
11. G. Adachi, I. Kato, J. Shiokawa and T. Ishino, *Kogyo Kagaku Zasshi* **69**, 2268 (1966).